The coordination of hydraulic and leaf photosynthesis properties is a critical feature underlying the spread and distribution of *Dasiphora fruticosa* in Qinghai-Tibet Plateau alpine meadows

Baoli Fan

baoli207@163.com

https://orcid.org/0000-0003-0918-4152

Nana Ding
Pengfei Gao
Ting ting Tian
Dongxia Ai
Yongkuan Wan
Miaojun Ma
Kun Sun

Research Article

Keywords: Alpine meadows, hydraulic conductivity, functional traits, shrub encroachment, resource conservative strategy, resource acquisition strategy

Posted Date: April 10th, 2024

DOI: https://doi.org/10.21203/rs.3.rs-4140458/v1

Abstract

Background and Aims

Global climate change and human-induced factors have resulted in shrub encroachment in the Qinghai-Tibet Plateau alpine meadows. Coordination among traits plays key role in plant adaptation to the environment. However, the mechanism by which the hydraulic and photosynthetic traits of shrubs are coordinated to adapt to different habitats on the Tibetan Plateau remain unclear.

Methods

Here, we assembled 23 root, stem and leaf traits, including hydraulic and photosynthetic traits, of a widely distributed shrub species, *Dasiphora fruticosa*, and tracked these against the degree of shrub encroachment (cover) on shady and sunny slope.

Results

We found that on shady slopes, *D. fruticosa* has enhanced hydraulic (K_L, K_S) and photosynthetic traits(A_a, A_m, g_s), while on sunny slopes it exhibits greater resistance capability (i.e high WD, more negative π^0). By optimizing its hydraulic and photosynthetic traits, *D. fruticosa* enable to flourish in two different environments. Furthermore, as influenced by STN, STP, root system of *D. fruticosa* in shady and sunny environments also adopted two different resource use strategies, such that the above-ground parts have a reverse pattern of resource acquisition compared to the below-ground parts. The relationships between stem and leaf hydraulics (i.e K_L, π^0, K_S) and economic traits (i.e LMA, RAD, SRL) drives the coupling of below- and above-ground resource of *D. fruticosa* in two environments.

Conclusion

Our study clearly shows the importance of hydraulics and leaf photosynthesis traits in governing shrub encroachment and provides useful values for predicting shrub encroachment as a response to climate change.

Introduction

Shrub encroachment is evidenced by an increase in abundance, coverage or biomass (Deng et al. 2021). The factors driving shrub encroachment are complex, and include factors such as overgrazing, grassland fire and increases in atmospheric CO_2 concentrations (Eldridge et al. 2021), all of which grant shrub species better access to environmental resources. this is an important ecological issue. In the ecologically fragile, high-altitude ecosystems of the Tibetan Plateau, climate warming is expected to result in domination by shrub species (Zhou et al. 2021). Although widely distributed across the Qinghai-Tibet Plateau, the total area covered by *Dasiphora fruticosa* shrubs is much less than the total area of *Kobresia* or alpine meadow (Li et al. 2013). Its presence affects below-ground biological communities

and productivity (Wang et al. 2018). It is generally considered that the tendency of specific woody species to is encroach related to their structural and functional traits (Eldridge et al. 2021). These can arise as short-term, rapid adaptions environmental variation (Funk et al. 2017). In addition, specific phenotypes with particular morphological or physiological traits may be selected over a longer period in response to environmental adaptations (Liu et al. 2023), all of which can help invasive plant species acquire more resources (Davidson et al. 2011; Liu et al. 2023). Thus, high phenotypic plasticity should provide a significant advantage enabling colonizing plants to thrive in a changing environment (Christiane et al. 2017). Shrub encroachment has been shown to impact a wide range of ecosystem goods, services and functions (Eldridge et al. 2021; Zhang et al. 2023), but little attention has been paid to the nature of specific morphological and physiological traits adopted during the shrub encroachment. A deeper understanding of these adaptive mechanisms could provide additional insight into means by which shrubs can maximizes resources in the face of climate change.

Where climate change results in decreased access to water then hydraulic functional traits that can enhance water transport capability efficiency and capacity or prevent loss of function, will acquire increased importance (Liang et al. 2019; Liu et al. 2019). For example, under drought conditions, some plant species have demonstrated increased resistance to cavitation under drought stress condition or improved their hydraulic conductivity or leaf turgor loss point (Bernhard et al. 2016; Liang et al. 2019). These are hydraulic functional traits with high plasticity. In addition, plants can cope with dry soil and atmospheric conditions by closing their stomata to avoid hydraulic failure, however, this results in a concomitant decline in carbon uptake (Joshi et al. 2022). Thus, stomata closing requires the coordination of plant hydraulics and photosynthetic (Xu et al. 2021; Zhu et al. 2018). Generally, fast-growing species should have high leaf photosynthetic capacity and K_{leaf} (leaf hydraulic conductivity), as contrasted with slow-growing species (Liu et al. 2019; Reich et al. 2014). This suggest that plants hydraulic traits are limited by the need to maintain stomatal conductance and gas exchange. Despite the importance of coordinated hydraulic and photosynthetic traits for plants in rapid growth, few studies have integrated stem and leaf hydraulics and leaf photosynthetic traits to explore on the spread and distribution of shrubs.

Studies of the coordination of functional traits have greatly advanced our understanding of responses to stress and how traits may be optimized to enhance a plant's resource use ability (Reich 2014). For instance, leaf economics spectrum (LES) describes the coordination of multiple leaf functional traits (Wright et al. 2004) and represents a trade-off strategy of plants, i.e a "low input-quick return" versus the "high input-low return" (Wright et al. 2005). The plant' s root economics spectrum (RES) is similar to the LES and represents a tradeoff between resource conservation and root nutrients exploration (Li et al. 2022). However, there are an increasing number of studies that have shown a weak relationship between root traits, which lead to multiple dimensions of fine-root trait variation (Ma et al. 2018; Silva et al. 2018). As described by Kong et al. (2019) the stele tissue and the tissues outside the stele, are two anatomical components of absorptive roots and follow an allometric relationship. Hence, root tissue density (RTD) and root diameter showed a nonlinear negative relationship. Currently, LES has been extended into the wood economic spectrum (WES) which describes the trade-offs between different species on a range of

woody traits related to plant carbon balance. These include wood density, a mechanical property of the stem (Eller et al. 2018). The coordination between below- and above-ground functional traits determines ecological strategies that plants make in response to local environment (Bricca et al. 2023; Carmona et al. 2021). The different organs are coordinated in a framework that represents the whole-plant economic spectrum (Liu et al. 2023). A recent study pointed out that *Artemisia* uses a whole-plant economics spectrum coordinating all organs (Liu et al. 2023). As above- and below-ground organs are exposed to different environmental stresses, and trait variation can lead to decoupling between organs and may potentially weaken the whole-plant economics spectrum (Medeiros et al. 2017; Zhou et al. 2024). In theory, water and nutrients will be transported through the root system, first, by rapid transport from the soil and then through the xylem to the leaves (Liu et al. 2023) where the coupling of CO_2 and water exchanges is controlled by plant adaptations to balance carbon gains and hydraulic risks (Joshi et al. 2022). Hence, stem and leaf hydraulic traits maybe play an important role in closely linking above- and below-ground activities. Recent studies have shown the sapwood to leaf area ratio is related to photosynthetic capacity (V_{cmax}) and leaf mass area (LMA), implying a balance between a plant's carbon investment in the water transport and carbon investment in building the leaf structure (Xu et al. 2021). However, Maréchaux et al. (2015) have reported a decoupling between leaf hydraulics and economic traits, thus there may be limited capacity from the whole-plant economic spectrum perspective to link plant hydraulics to economic traits of other organ as an adaptive strategy in the face of climate change (Maréchaux et al. 2015; Xu et al. 2021).

The effect of shrub encroachment ecosystem structure and function have been extensively studied, however, the adaptive significance of below- and above-ground functional traits and their role in different ecotype formation of *D. fruticosa* has often been ignored, particularly with respect to highly variable hydraulic traits (Anderegg et al. 2014). These are important for explaining species distributions and predicting plant responses to climate change. Hence, we measured and compared functional traits of fine roots (RES), leaves (LES) and wood (WES), including hydraulics traits of *D. fruticosa* grown on shady and sunny slopes. We also explored the relationships between shrub encroachment and these traits. We aimed to determine how shrubs adjust their above- and below-ground resource strategies to cope with different habitats and the role of hydraulic traits in shrub encroachment. We therefore tested following hypotheses: (1) that coordination of hydraulic and leaf photosynthetic traits plays a key role enabling distribution across both shady and sunny slope shrub *D. fruticosa*; (2) that resource use strategies of above- and below-ground organs of *D. fruticosa* growing on shady and sunny slopes are relatively independent; (3) that stem and leaf hydraulic traits promote coupling of above- and below-ground resources in *D. fruticosa* to form a whole-plant economic spectrum.

Materials and methods

Study area

The studies were carried out in the 'Gannan Tibetan Autonomous Prefecture, located near Hezuo city, on the northeastern Qinghai-Tibetan Plateau, China (E 102°88', N34°94', at an average elevation of 2900m).

The area has a typical plateau continental climate with long daylight hours and strong radiation. The average annual precipitation is 545mm, with most falling between August and September. The annual mean air temperature is 2℃, with a monthly minimum of -23°C in January and a monthly maximum of 28°C in July. Frosts may occur at any time throughout the year. Meteorological data in the study regions were collected using grid data covering CRU TS4.04 (LAND) from 1901 to 2020. Soils were classified as alpine meadow soils. The vegetation type mainly consisted of *D. fruticosa* shrubs, which is a typical alpine shrub meadow (He et al. 2016). Other herbaceous species, included *Kobresia myosuroides*, *Elymus nutans, Kobresia humilis, Kobresia capillifolia, Stipa aliena, Potentilla anserina etc.*

Experimental design

In September 2022, sampling was carried out in two habitats (shady and sunny slopes), carefully matched to have essentially similar micro-topography, soil depth, origin of soil parent materials and minimal anthropogenic disturbance. We randomly placed three 5m×5m quadrants, approximately 20m apart, in each habitat. Within each quadrant, we selected similar base diameter (Table S1). Shrub height, density were also matched. In this study, we used the proportion of shrub cover as a measure of shrub encroachment (Liao et al. 2018) (Table S1). We then selected three healthy and similarly sized individual shrubs for collection of root and leaf samples in each plot (corresponding to subsequent photosynthesis measurements). At least fifteen intact fine-root in each plot were excavated, and five soil samples were collected with a soil auger at 0-20 cm depth in each habitat. To minimize differences due to sampling position, the sampled soils were mixed to obtain a composite sample. After collection, the fresh leaf, root and soil samples were packed in ice for transport to the laboratory.

Soil sampling and measurements

Soil moisture was measured in samples collected over a minimum of six consecutive sunny days. After picking out the root and coarse stone, the soil samples of each quadrant were divided into two parts. One part was packed into an aluminum box for transport to the laboratory where soil water content was measured after 24h drying in an oven at 105°C. The other part was brought back to the laboratory in plastic bags for determination of the soil nutrients. These soil samples were air-dried in the laboratory, passed through a 1 mm sieves and used for analysis of soil pH which was measured in a 1:1 (v/v) soil water solution. Soil was passed through an additional 0.25mm sieve before determining soil organic carbon (SOC), soil total phosphorus (STP) and soil total nitrogen (STN). SOC was determined by the potassium dichromate and sulfuric acid oxidation method (Liu et al.2023). The sulfuric acid-perchloric acid digestion was used for both STN and STP. STN was then determined by the indophenol blue spectrophotometry and STP by the molybdenum antimony anti-colorimetric method. Soil water content (SWC, %) was determined by the oven dried method. Soil water content and total P measurement were performed as described by Fan et al. (2023).

Root functional traits

We measured fine-root traits associated with the root economic spectrum. These included specific root length (SRL; m/g), root average diameter (RAD; mm), and root tissue density (RTD; g/cm^3) (Kong et al. 2019).The study methodology broadly followed Liu et al. (2023). Fine roots (<2mm) were carefully cleaned in water. Then root samples were selected and scanned (KingHun Optoelectronic Technology Co., Ltd). Then total length and average diameter was measured with a Vernier scale. The total volume of fine roots was measured by the drainage method. Root sample were oven-dried at 60°C for 48 h to determine the dry mass. SRL was calculated as fresh root length / dry mass. RTD was calculated as dry mass/ fine roots volume. Specific root area (SRA, cm^2/g) was calculated as fine root surface area/ dry mass.

Leaf functional traits

Photosynthetic traits, including net photosynthetic rate (P_n), intercellular CO_2 concentration (C_i), transpiration rate (T_r) and stomatal conductance (g_s), were all measured across the field sites. Three individual plants were selected from each habitat. Three healthy, intact leaves were randomly selected from these individuals. Measurements were determined using a portable photosynthesis system (GFS-3000, Heinz Walz GmbH, Effeltrich, Germany) from 9:00-11:30h on continuous sunny days. Photosynthetically active radiation, temperature and CO_2 concentration were settled at 1500μmol·m^{-2}·s^{-1}, 390umol.mol^{-1}, 12°C. Water use efficiency (WUE) was expressed by the following formula: net photosynthetic rate (Pn) / transpiration rate (Tr).

Leaf traits measured were leaf mass per area (LMA), leaf N and P content. After photosynthesis measurements, we collected leaf samples to take back to the lab for subsequent measurements. We randomly selected and weighed (accuracy of 0.0001g) at least 100 mature and healthy leaves and leaf area was quantified using ImageJ software after scanning (KingHun Optoelectronic Technology Co., Ltd). The leaves were oven-dried at 60°C for 48h and weighed to obtain the leaf dry weight. The dried samples were then powdered in stainless steel mill for leaf N and P content analysis. Leaf mass per area (LMA) was expressed as leaf dry weight (LDW)/leaf area (Rosas et al. 2021). Samples for leaf N and P content were all subject to H_2SO_4-H_2O_2 digestion. Subsequently, leaf N content was measured by the indophenol blue spectrophotometry. Leaf P content was measured by the molybdenum-antimony anti-colorimetric method (Forestry Industry Standards of the People's Republic of China; LY/T 1269–1999).

The maximum photosynthetic rate per unit leaf dry weight (A_m, nmol. g^{-1}. s^{-1}) was calculated as maximum photosynthetic rate per unit leaf area (A_a, umol.m^{-2}. s^{-1}) /leaf mass per area (LMA). Photosynthetic nitrogen use efficiency (PNUE, umol. g^{-1}. s^{-1}) was calculated as A_m / $N_{mass\text{-}leaf}$. Photosynthetic phosphorus use efficiency (PPUE, umol. g^{-1}. s^{-1}) was calculated as A_m / $P_{mass\text{-}leaf}$.

Stem and leaf hydraulic traits

In each habitat, at least ten branches from the upper canopy and in close proximity to the branches used to determine photosynthetic traits, were selected in the morning for measurement of hydraulic traits in the laboratory. The branches were immediately put in water and the ends of the branches were re-cut. Measurements were made using potassium chloride (20 mmol L^{-1}) solution and ~5 KPa hydrostatic pressure with the distal end of the branch connected to the pipette to obtain a steady flow rate. The hydraulic conductivity (K_h, g m s^{-1} MPa^{-1}) was calculated as follows: $K_h=F/(dp/dx)$, where dp/dx (MPa m^{-1}) is the pressure gradient along the length of the segment and F (g s^{-1}) is the flow of water through the stem section per unit time. After hydraulic conductivity was determined, distal leaves from each branch were collected and scanned (KingHun Optoelectronic Technology Co., Ltd) and leaf area was quantified by ImageJ software. Total wood and heartwood diameter were measured with a vernier scale. Then sapwood area was measured by total wood and heartwood diameter. Stem sapwood specific conductivity (K_s, g m^{-1} s^{-1} MPa^{-1}) was calculated as the hydraulic conductivity (K_h, g m s^{-1} MPa^{-1}) / the sapwood area (A_s, cm^2). Leaf specific hydraulic conductivity (K_L, g m^{-1} s^{-1} MPa^{-1}) was calculated as the hydraulic conductivity (K_h, g m^{-1} s^{-1} MPa^{-1}) / the distal leaf area (A_L, cm^2). The Huber value (HV) was determined by the sapwood area (A_s, cm^2) / the distal leaf area (A_L, cm^2).

Stem vulnerability curve

Following the method of Sperry et al. (1988), we sampled 60-70 mature and health branches from two habitats to measured stem vulnerability curves (VCs). Briefly, sampling was done before sunrise. After cutting the branches from shrubs, they were sprayed with water and the cut area wrapped with damp papers to prevent air from entering the xylem and causing artificial embolism. They were then placed into black plastic bags for transport back to the laboratory. Branches with different water potential gradients were measured by bench drying methods. When a selected branch reaches a certain water potential gradient, they were then were covered with black plastic bags to balance the water potential. When the difference in water potential between two branchlets was <0.2 MPa, the average of two branchlet was assumed to be the xylem water potential. After 5 cm was cut from the basal ends to release tension, the segments were connected to a hydraulic measurement system with ~5KPa hydrostatic pressure and 20 mmol L^{-1} KCL solution. Then the actual hydraulic conductivity (K_i, g m s^{-1} MPa^{-1}) was determined. The maximum hydraulic conductivity (K_{max}, g m s^{-1} MPa^{-1}) was determined again after flushing the segment with 150 KPa pressure KCl solution for about 30 min. The PLC (the percentage of loss hydraulic conductivity, %) was expressed by the formula: $PLC(\%)=(K_{max}-K_i)/K_{max}\times100\%$. The vulnerability curves were plotted using PLC% as a function of the xylem water potential, and then fitted by an exponential sigmoid function: $PLC\%=100/\{1+\exp^{a(\Psi_i-b)}\}$, where Ψ_i is xylem water potential, a is the maximum slope of the curve and b is the xylem water potential at 50 % loss of hydraulic conductivity (P_{50}), which can reflect the resistance of branches to embolism.

Leaf pressure-volume curve

From the two habitats, leafy branches were randomly sampled from each of five individual shrubs, then quickly wrapped in a black plastic bag to prevent leaf transpiration and transported back to the laboratory. Before measurement, branches were rehydrated to saturation until Ψ_{min} approached 0 MPa. Branches were then weighed and put on the table to dry for a certain time when Ψ was remeasured and the leafy branches again weighed, until Ψdid not decrease significantly (Aritsara et al. 2022). Leaf area (LA) of each branchlet was determined after scanning using ImageJ software. Dry weight (DW) was measured in an oven at 70℃ for 72 h. The relative leaf water content (RWC, %) and RWC were expressed by the following formula: RWC=(FW-DW)/(SW-DW) ×100%; RWC_{tlp}= 100-RWC. Then using 100-RWC_{tlp} and the corresponding -1/Ψ to make the P-V curve, modulus of elasticity(ε) and leaf turgor loss point water potential(π^0) and were determined from the P-V curve (Bartlett et al. 2012).

Wood density and Minimum water potential

Segments (3-5 cm) selected for hydraulic conductivity measurement were used to measure the sapwood density (WD, g cm^{-3}) following the methods of Hacke et al. (2000). Bark and pith material were separated from segments and Archimedes' drainage method was used to measure the volume of the fresh sapwood (V, cm^3). The sapwood sample was dried in an oven at 75°C for 72 h to determine the dry mass(W, g), and then used for determination of WD. WD was determined by dividing the dry mass by the volume of fresh sapwood.

On a sunny day, five branches were selected between 12:00 noon-13:00 pm and quickly wrapped in a black plastic bag, and immediately taken to the laboratory. Subsequently minimum water potential (Ψ_{min}) was determined with a pressure chamber (Model 1505D, PMS Instrument Company, Albany, USA).

Data analysis

All traits were tested for normality and all original data were log_{10}-transformed. One-way ANOVA and the least significant difference (LSD) method were used to determine community structure traits and soil nutrient difference. Differences in branch hydraulic structure and photosynthetic capacity relationships between shady and sunny slopes of *D. fruticosa* were compared with independent-samples t-test. Pearson correlations and linear regression analysis were performed for pairwise combinations of traits. Additionally, to assess the relationships between fine root functional traits and soil variables, we conducted stepwise multiple regressions analysis. To assess relationships between shrub encroachment and functional traits, PCA was performed using all functional traits and vegetation cover. All statistical analyses were performed using SPSS 26.0 software, and figures were drawn with Origin 2022.

Results

Differences in functional traits of *D. fruticosa* between two habitats

Differences in the fine root functional traits

Compared to the shady slope, the SRL and SRA on the sunny slope were larger by 117.5% and 7.5%, respectively (Fig.1a 1c). Compared to the sunny slope, the RAD and RTD on the shady slope were significantly larger (p<0.05) by 60% and 56.7%, respectively (Fig.1b 1d). Results clearly indicated significant differences between the SRL and RAD on the shady and sunny slopes (p<0.05) (Fig.1b 1c).

Differences in the leaf functional traits

Our results demonstrated that LMA, N_{mass}, P_{mass} changed significantly(p<0.05) between the shady and sunny slopes (Fig. 2a, 2b, 2c). Additionally, N_{mass}, P_{mass}, PPUE, PNUE on the shady slope were greater by 54.44%, 89.38%, 14.34% and 17.14% over the sunny slope (p<0.05) (Fig. 2b, 2c, 2d, 2e). LMA on the shady slope was smaller by 42.31% compared with sunny slope (p<0.05) (Fig. 2a).

Differences in population characteristics and soil physicochemical properties of *D. fruticosa* in different habitats

Our result indicated that plant density, height and cover changed significantly (p<0.05) between the two habitats. Density, height and cover of *D. fruticosa* on the shady slope were 2.46, 0.19 and 7.85 times higher than the sunny slope (Table S1). One-way AVONA analysis also showed that shady slopes have higher SOC, STP, STN, pH, demonstrating significant differences (p<0.05) between the shady and sunny slopes (Table S2).

Differences in branch and leaf traits of *D. fruticosa* between two habitats

Differences in the branch vulnerability curve between shady and sunny slopes

From the stem vulnerability curves for the shady and sunny slopes, it can be seen that the P_{50} value is -0.97MPa on shady slope (Fig. 3a), and -1.43MPa on the sunny slope (Fig. 3b). This results indicate a higher embolism resistant capacity for plants growing on the sunny slope compared to those on the shady slope.

Differences in hydraulic and photosynthetic traits

Leaf and stem traits vary significantly between the sunny and shady slopes. K_L, K_S, HV, π^0, Ψ_L, A_a, A_m, T_r, P_n, g_s on the sunny slope were significantly lower than for the shady slope (p<0.05) (Table 1). However, ε and WD on the shady slope was significantly lower than for the sunny slope (p<0.05). WUE on the shady slope was also lower than for the sunny slope(p>0.05)(Table 1).

Table 1 Differences in hydraulic and photosynthetic traits between shady and sunny slope (mean ± SE). See Abbreviations for the following traits.

Traits	units	Shady slope	Sunny slope	t	*p*
KS	g m-1 s-1 MPa-1	26.60±9.70	11.64±3.52	-5.240	0.000
K_L	g m-1 s-1 MPa-1	1.10±0.31	0.03±0.02	-12.441	0.000
HV	cm2 cm-2	4.59±1.85	2.62±1.92	-2.967	0.012
WD	g cm-3	0.63±0.09	0.71±0.07	2.767	0.011
π0	MPa	-0.59±0.14	-1.03±0.17	-7.406	0.000
ε	MPa	15.71±2.47	22.46±2.40	7.192	0.000
ΨL	MPa	-1.79±0.48	-2.10±0.31	-1.996	0.057
A_a	$umol.m^{-2}. s^{-1}$	21.64±1.10	15.74±1.28	-12.867	0.000
A_m	$nmol. g^{-1}. s^{-1}$	222.49±75.01	118.76±28.58	-4.675	0.000
Tr	$mmol.m^{-2}. s^{-1}$	4.69±0.29	2.93±0.46	7.199	0.000
P_n	$umol.m^{-2}. s^{-1}$	13.25±0.67	8.76±1.30	6.850	0.000
g_s	$mol.m^{-2}. s^{-1}$	0.49±0.03	0.28±0.07	5.925	0.000
WUE	$umol. mmol^{-1}$	2.82±0.26	3.13±1.01	1.111	0.277
$C_i:C_a$	/	0.88±0.01	0.86±0.03	1.270	0.240

Soil factors influencing vegetation cover and variations in fine-roots functional traits

Our results indicated that the presence of *D. fruticosa* shrubs was associated with significant differences in soil nutrients (Fig. S1). SWC, SOC, STN, STP and pH were all positively related to the degree of shrub cover (Fig. S1).

The PCA showed that *D. fruticosa* in different habitats are mainly affected by SRL and RAD (Fig. 4, Table S3). In addition, the stepwise multiple regression analyses showed that STN and STP were determined as the most affected factors on RAD and SRL (Table 2).

Table 2 Summarized results of the stepwise multiple regression analyses with root functional traits (SRL, SRA, RAD, RTD) as dependent variables and soil nutrients (SOC, STP, STN, SWC, pH) as independent variables. Coefficients (β) and *P-values* for each independent variable as well as coefficient of determination (R^2) and *P-values* and *F-values* in each model are shown. STP and STN were predictors and SWC, SOC and pH were excluded variables in model. See Abbreviations for soil properties.

Independent	SRL		RAD		SRA		RTD	
variable	*β*	*P-values*	*β*	*P-values*	*β*	*P-values*	*β*	*P-values*
STN	-0.098	0.776	0.666	**<0.001**	0.562	0.163	-0.91	0.019
SWC	-0.024	0.3	0.124	0.458	-0.357	0.136	0.109	0.614
STP	-0.451	**0.018**	0.235	0.41	-0.979	0.085	0.907	0.084
SOC	-0.127	0.58	-0.045	0.81	-0.464	0.177	0.641	0.049
pH	0.435	0.248	-0.23	0.92	0.929	0.096	-0.467	0.354
F-values	6.931		19.977		1.05		1.941	
R^2	0.172		0.422		0.01		0.153	
P-values	0.018		<0.001		0.415		0.13	

Relationships between functional traits

Our result showed that K_L and Ks were positively related to A_a, A_m, P_{mass}, N_{mass}, g_s, and RAD (p<0.05) (Fig. 5e-l) and negatively correlated with SRL, WD, RWC_{tlp}, ε, π^0 (Table S4). Whereas WD was positively correlated with ε, π^0 (p<0.05) (Table S4). SRL was negatively correlated with RAD, P_{mass} and RTD (p<0.01) (Fig. 5b-5d). There was no significance correlation with RAD and RTD (p>0.05) (Table S4). Additionally, SRL was negatively related to A_a and g_s (p<0.05), and RAD was positively related to P_{mass}, A_a, A_m and g_s (p<0.05) (Table S4). LMA was negatively related to K_L, K_S, A_m, PPUE, PNUE (Fig 5n-5p) and positively correlated with RWC_{tlp}, ε, π^0(p<0.05) (Fig. 5m) (Table S4).

Principal component analysis between functional traits and shrub encroachment of different habitats

The Principal Component Analysis (PCA) indicated that PC1 and PC2 explained 58.50% of the total variance. The first PC accounted for 43.5% of the total variation, the second PC accounted for 15.0% of the total variation (Table 3). The PC axis 1 was loaded by Cover, K_L, K_S, HV, A_a, A_m, P_n, g_s, P_{mass}, N_{mass}, PPUE, PNUE, RAD, RTD. the PC axis 2 was loaded by π^0, ε, RWC_{tlp}, Ψ_L, SRA, SRL, LMA, WD and WUE (Fig. 6). *D. fruticosa* on the shady slope was clustered to the right of the PCA plot, whereas *D. fruticosa* on the sunny slope was clustered to the left of the PCA plot. These results indicated that *D. fruticosa* shrubs on shady slopes were positively correlated with K_L, K_S, A_a, A_m, g_s, P_{mass}, whereas *D. fruticosa* shrubs on sunny slopes were postively correlated with π^0, ε, RWC_{tlp} (Fig. 6). Additionally, tested traits of *D. fruticosa* on sunny and shady slopes were distributed along the diagonal line between the PC axis 1 and 2, meaning that the functional traits of different organs together determine the different adaptive strategies by which *D. fruticosa* are able to flourish in different habitats (Fig. 6).

Table 3 The Eigenvalue of each axis of PCA ordination of different habitats and correlation coefficients of functional traits with each axis

Principal component	PC1	PC2	PC3
Eigenvalue	10.00	3.45	2.35
Percentage of total variance (%)	43.50	15.01	10.22
Cumulative percentage (%)	43.50	58.50	68.72
Factor loading			
K_L	0.30	0.07	-0.02
K_S	0.22	0.13	-0.11
WD	-0.16	-0.05	0.15
HV	0.20	-0.01	0.08
RWC_{tlp}	-0.23	0.20	-0.08
π^0	-0.29	0.09	0.15
ε	-0.26	-0.02	0.28
Ψ_L	-0.15	0.20	-0.26
SRL	-0.18	-0.30	-0.10
SRA	-0.06	-0.36	-0.15
RAD	0.19	0.13	0.17
RTD	0.02	0.27	-0.07
N_{mass}	0.22	-0.14	-0.39
P_{mass}	0.25	0.22	-0.22
LMA	-0.17	0.35	0.11
A_a	0.30	0.02	0.13
A_m	0.26	-0.26	-0.04
PNUE	0.11	-0.20	0.39
PPUE	0.04	-0.49	0.17
g_s	0.26	0.11	0.21
WUE	-0.04	-0.08	-0.21
C_i:C_a	0.15	0.12	0.47

Discussion

The role of hydraulic and leaf photosynthetic traits in shrub encroachment of *D. fruticosa*

Our study showed that photosynthetic capability is significantly and positively correlated with the leaf hydraulic conductivity at a whole-plant level (Fig. 6), as plant water supply and ability to deliver water to the leaf canopy determines the photosynthetic capacity. When trees grow on sites providing sufficient water for photosynthesis, growth is usually enhanced and a high K_L, ensures a faster rate of gas exchange (Li et al. 2021). On shady slopes with an abundance of resources, *D. fruticosa* had high water conductivity and photosynthetic capability (Fig. 6) strengthening their competitive advantage in this habitat. This also accords with a recent global scale study that identified a significant correlation between maximum tree height and number of hydraulic features (Liu et al. 2019). The PCA between leaf, fine-root, stem traits and shrub encroachment of the two habitats reveals K_L, A_a, g_s, bulk modulus of elasticity(ε) and leaf turgor loss point(π^0) were significantly correlated with vegetation coverage (Fig. 6), indicating coordination of hydraulic and photosynthetic factors in the widespread distribution of *D. fruticosa*. Thus, *D. fruticosa* on shady slopes grow faster and have a higher degree of shrub encroachment compared to the sunny slopes. This supports our first hypothesis. High wood density identified as a factor in species embolism resistance (Han et al. 2022). and in support of this we have found that *D. fruticosa* on sunny slopes have high wood density, low water conductively rates and photosynthetic capability. This is because wood density is correlated with hydraulic efficiency (Eller et al. 2018). In addition, the minimum leaf water potential (Ψ_L) and leaf turgor loss point(π^0) could be used to predict the plant response to drought. In our study, wood density is correlated with leaf turgor loss point (π^0), bulk modulus of elasticity(ε) and minimum penitential(Ψ_L) (Table S4). *D. fruticosa* on sunny slopes have lower π^0 and minimum leaf water potential and greater xylem resistance to embolism and ability to resist leaf dehydration and plants could maintain stomatal conductance, allowing photosynthesis under lower water availability (Zhu et al. 2018). As a result, although sunny slopes have less soil water and nutrients than shady slopes, *D. fruticosa* shrubs also able to grow on sunny slopes.

When considering the trade-off between hydraulic efficiency and safety, fast-growing species, have higher hydraulic conductivity and carbon assimilation at the cost of increased risk of hydraulic failure under the influence of global climate change, mainly in terms of larger P_{50} values (Han et al. 2022). Whereas *D. fruticosa* on shady slopes had a larger P_{50} value. When *D. fruticosa* on shady slopes experienced water stress, it was more likely to develop embolism due to its weaker xylem resistance, resulting in hydraulic failure and death. However, leaf turgor loss point (π^0) has been shown to have phenotypic plasticity under changing environment (Pritzkow et al. 2019). This provides not only potentially increased hydraulic efficiency, but also increased hydraulic safety when plant species are confronted with particularly unfavorable conditions. Our study also showed that π^0 is strongly correlated with plant cover (Fig. 6). Hence, the presence of this indicator may alleviate this problem of low resistance to shady slopes(Santiago et al. 2018).

Coupling relationships between functional traits of above- and below-ground organs in *D. fruticosa*

LMA is generally considered to be related to leaf carbon-fixation capacity and plant-growth strategies (Rosas et al. 2021) and there is a significant negative relationship between LMA and K_L, A_m (Table S4), However, *D. fruticosa* on sunny slopes has thicker leaves and lower K_L which is consistent with a longer diffusional pathways in the mesophyll, which increases water movement resistance outside leaf xylem and decreases its hydraulic conductivity (Xu et al. 2021). The results also showed that LMA was also significantly positively related to π^0, and significantly negatively correlated to leaf N and P content (Table S4). Also, wood density was negatively correlated with π^0, suggesting that conservative leaves may have relatively dense wood. This result is no consistent with Mediavilla et al. (2020) who found the wood economic spectrum and the leaf economic spectrum are independent. The cause of this difference in coordination between hydraulic and economic traits may be applicable only to plants that are distributed over small scale environmental gradients. *D. fruticosa* on sunny slopes and leaves with lower nutrients content tend to have a more negative π^0 and thicker leaves. The devotion of more resources to building leaf structures, reduces the resources available for photosynthetic and respiratory functions, resulting in better xylem-cavitation resistance and drought tolerance (Maréchaux et al. 2020); a conservative strategy of above-ground functional traits. Thus, leaf structure (i.e LMA) is related to carbon allocation and to water transport (Xu et al. 2021), confirming that increased leaf turgor maintenance is related to leaf carbon investment (Zhu et al. 2018). Our results are indicative of clear differences with respect to carbon gain and water use strategies between *D. fruticosa* on shady and sunny slopes (Table 1). There is a strong positive relationship between hydraulic conductivity (K_L, K_S) and leaf photosynthetic capacity (A_a, g_s) (Fig. 5), evidence for coordination between water transport capacity and leaf CO_2 assimilation (Liu et al. 2019). Higher hydraulic conductivity and photosynthetic capacity enable *D. fruticosa* on shady slopes to have faster growth. This is contrary to the situation pertaining to *D. fruticosa* on sunny slopes (i.e fast acquisition strategy).

The fine roots system, which is in direct contact with the soil environment, allows plants not only take up water and nutrients from the soil for plant growth, but to also respond to number of soil factors. In our study, *D. fruticosa* growing on sunny slopes is limited by soil moisture and nutrients compared to shady slopes. A stepwise regression further indicated that STN and STP were the main soil factors affecting SRL and RAD (Table 2). In addition, SRL was significantly and negatively correlated to RAD (Table S4), which suggests a coordinated variation in root acquisition strategies (Li et al. 2019). These two root traits represent the ability of plants to transport and absorb nutrients. Thus, smaller diameter and longer fine roots have increased the soil contact with the volume and can absorb more soil nutrients, in turn promoting growth. *D. fruticosa* growing on sunny slopes found to have greater SRL and lower RAD, enabling plants to grow in a relatively poor soil habitat. This is compatible with the findings of Liu et al. (2023) who found that plants growing in phosphorus-limited soils tend to have finer and deeper roots. It represents an effective strategy in nutrient-poor environments (Bricca et al. 2023). In contrast, *D. fruticosa* growing on shady slopes tend to have increased root diameters. Thicker roots have been reported to be linked to resource conservative strategies. Thus, thicker roots have higher root dry mass

and lignin content, and display greater root life span (Li et al. 2019). The increase in root diameter also provides more space for mycorrhizal colonization, which in turn allows an increased acquisitive potential for the larger root system (Li et al. 2019). However, we found that there is no linear relationship between RAD and RTD (Table S4). An investment in root dry matter could result in longer root lifespan, but based on the anisotropic relationship with root anatomy, we suggest that RAD plays a dominate role in root dry matter and lifespan rather than RTD (Kong et al. 2019). This combination of multiple root traits of *D. fruticosa* improves the adaptation of the root system to different environments, allowing it to adopt different resources use strategies. Over all, these findings also support our second hypothesis, that is, the above- and below-ground organs of *D. fruticosa* on shady and sunny slopes adopted opposite resource use patterns, i.e. above-ground organs adopted a relatively fast acquisitive strategies (or conservative strategy) and below-ground root system showed a relatively conservative strategies (or acquisition strategy) to adapt to soil nutrients.

A combined consideration of both above- and below-ground functional traits enables better prediction of plant growth and will improve our understanding of the underlying processes by which shrub encroachment occurs. Specifically, RAD are significantly positive related to K_s, K_L, g_s, A_a, P_{mass} (Table S4). In contrast, SRL are significantly negative related to K_L, g_s, A_a (Table S4). Thicker root systems usually exhibit slower growth rates due to their relatively small surface area, but we have found that *D. fruticosa* on shady slopes are fast-growing, which may be due to mycorrhizal fungi that enhance the uptake of soil resources (Kong et al. 2019; Bergmann et al. 2020). The close linkage of fine root traits primarily with stem and leaf hydraulics and leaf economic traits, results in trade-off relationships between resource conservation (or acquisition) and fast growth (or slow growth) (Reich et al. 2014): a whole-plant economic spectrum of *D. fruticosa*, rather than coordinated combinations of above- and below-ground organ traits. Thus, *D. fruticosa* can exhibit rapid growth in two habitats, using opposite trait combinations to maximize access to resource above- and below-ground. These results also confirm the third hypothesis. It is important to note that the apparent positive correlation with SRL was less than the accepted level of significance. This result is compatible with the findings of Liu et al. (2023), and with SRL associating with mycorrhizal fungi. Roots outsource nutrient uptake to root mutualistic symbionts, resulting in root trait variation (Bergmann et al. 2020). Root trait variation weakens coordination among organs. Thus, different organs have different strength of coordination and adaptation strategies to specific habitats. The reasons for this coordination also may be the continuous anatomical structures of stems, roots and leaves are very different (Liu et al. 2023).

Conclusion

Our study demonstrates that the high hydraulic conductivity and leaf photosynthetic traits of *D. fruticosa* on shady slopes are coordinated with each other. The above-ground organs adopt a resource acquisition strategy that leads to more severe shrub encroachment. However, efficient water transport capacity is accompanied by the risk of hydraulic failure, which is compensated to some extent by the drought tolerance indicator of *D. fruticosa* on shady slopes. In contrast, *D. fruticosa* on sunny slopes is highly

resistant to embolism with its above-ground adoption of a resource conservative strategy. At the same time, the root system of *D. fruticosa* adopted the opposite resource use to the above-ground part to adapt to soil heterogeneity. Thus, stem and leaf hydraulics allow for the existence of trade-offs between above- and below-ground resource use patterns, culminating in a whole-plant economics spectrum of *D. fruticosa*, and an effective adaptive strategy to deal with climate change.

Abbreviations

Fine root functional traits	SRA	Specific root area
	RAD	Root average diameter
	SRL	Specific root length
	RTD	Root tissue density
Leaf functional traits	LMA	Leaf mass area
	N_{mass}	Leaf nitrogen content
	P_{mass}	Leaf phosphorus content
	PPUE	Photosynthetic phosphorus use efficiency
	PNUE	Photosynthetic nitrogen use efficiency
Hydraulic and wood traits	K_S	sapwood-specific hydraulic conductivity
	K_L	leaf-specific hydraulic conductivity
	WD	sapwood density
	HV	Huber value
	ε	bulk modulus of elasticity
	π^0	turgor loss point water potential
	Ψ_L	minimum leaf water potential
Leaf photosynthetic traits	WUE	photosynthetic water use efficiency
	g_s	stomata conductance
	Ci:Ca	Intercellular CO_2 concentration: intracellular CO_2 concentration
	A_m	maximum leaf mass-based photosynthesis rate
	A_a	maximum leaf area-based photosynthesis rate
	P_n	net photosynthetic rate
	T_r	Leaf transpiration rate
Soil physicochemical properties	STN	Soil total nitrogen
	STP	Soil total phosphorus
	SOC	Soil organic carbon
	SWC	Soil water content

Declarations

Acknowledgements

All traits and soil data collection completed by the Gansu Gannan Grassland Ecosystem National Observation and Research Station. This research was supported by the National Natural Science Foundation of China (32260271, 32201525), the Gansu province's Key Research and Development Plan (21YF5NA069), the Long yuan Talent Youth Innovation and Entrepreneurship Team project (2022LQTD56), the Key Laboratory of Eco-functional Polymer Materials of the Ministry of Education (YDZX20216200001007), the Foreign Expert Introduction Special Project of Gansu Province (22JR10KA010).

Author Contributions

B.L.F. designed the study, revised the first draft and led the writing on subsequent revisions. N.N.D. collected and analyzed the data and wrote the first draft. Data from the field study was also collected by P. F. G., T.T.T., D. X.A., Y. K.W., M. J. M. and K. S. provided input regarding the study design. All authors approved the final version of the manuscript.

Data Availability

The datasets generated during and analyzed during the current study are available from the corresponding author on reasonable request.

Competing Interests

The authors have no relevant financial or non-financial interests to disclose.

References

1. Anderegg WRL (2014) Spatial and temporal variation in plant hydraulic traits and their relevance for climate change impacts on vegetation. New Phytologist, 205(3), 1008-1014. https://doi.org/10.1111/nph.12907.
2. Aritsara ANA, Wang S, Li BN, Jiang X, Qie YD, Tan FS, Zhang QW, Cao KF (2022) Divergent leaf and fine root "pressure–volume relationships" across habitats with varying water availability. Plant Physiology, 190(4), 2246-2259. https://doi.org/10.10 93/plphys/kiac403.
3. Bernhard S, Florian K, Sylvain D, Steven J, Hilmar MH, Régis B, Yann C, Christoph L (2016) How adaptable is the hydraulic system of European beech in the face of climate change-related precipitation reduction? New Phytologist, *210*(2), 443-458. https://doi.org/10.1111/nph.13798.
4. Bergmann J, Weigelt A, Van DPF, Laughlin DC, Kuyper TW, Guerrero-ramirez N, Valverde-barrantes OJ, Bruelheide H, Freschet GT, Iversen CM, Kattge J, Mccormack ML, Meier IC, Rillig MC, Roumet C, Semchenko M, Sweenney CJ, Ruijven JV, York LM, Mommer L (2020) The fungal collaboration

gradient dominates the root economics space in plants. Science Advances, 6(27). http://doi.org/10.1126/sci adv.aba3756.

5. Bricca A, Sperandii MG, Acosta ATR, Montagnoli A, Bella GL, Terzaghi M, Carboni M (2023) Above- and belowground traits along a stress gradient: trade-off or not? Oikos, e010043. https://doi.org/10.1111/oik.10043.
6. Bartlett MK, Scoffoni C, Sack L (2012) The determinants of leaf turgor loss point and prediction of drought tolerance of species and biomes: a global meta-analysis. Ecology letters, 15(5), 393-405. https://doi.org/10.1111/j.14610248.2012.017 51.x.
7. Carmona CP, Bueno CG, Toussaint A, Träger S, Díaz S, Moora M, Alison DM, Pärtel M, Zobel M, Tamme R (2021) Fine-root traits in the global spectrum of plant form and function. Nature, (597) 683–687. https://doi.org/10.1038/s41586-021-03871-y.
8. Carvajal DE, Loayza AP, Rios RS, Delpiano CA, Squeo FA (2019) A hyper-arid environment shapes an inverse pattern of the fast–slow plant economics spectrum for above-, but not below-ground resource acquisition strategies. Journal of Ecology, *107*(3), 1079-1092. https://doi.org/10.1111/13652745.130 92.
9. Christiane R, Marlén G, Annett L, Jens S, Alexandra W, Nina B, Ernst-Detlef S, Bernhard S (2017) Trait means, trait plasticity and trait differences to other species jointly explain species performances in grasslands of varying diversity. Oikos, *127*(6), 865-865. https://doi.org/10.1111/oik.04815.
10. Deng Y, Li X, Shi F, Xia H (2021) Woody plant encroachment enhanced global vegetation greening and ecosystem water-use efficiency. Global Ecology and Biogeography, 30(12), 2337-2353. https://doi.org/10.1111/geb.13386.
11. Davidson, AM, Jennions, M, Nicotra, AB (2011) Do invasive species show higher phenotypic plasticity than native species and, if so, is it adaptive? A meta-analysis. Ecology Letters, 14, 419-431. https://doi.org/10.1111/j.1461-0248.20 11.01596.x.
12. Eller CB, Barros FD, Bittencourt PRL, Rowland L, Mencuccini M, Oliveira RS (2018) Xylem hydraulic safety and construction costs determine tropical tree growth. Plant, Cell & Environment, 41(3): 548-562. https://doi.org/10.1111 /pce. 13106.
13. Eldridge DJ, Ding JY (2021) Remove or retain: ecosystem effects of woody encroachment and removal are linked to plant structural and functional traits. New Phytologist. *229*(5), 2637-2646. https://doi.org/10.1111/nph.17045.
14. Funk JL, Larson JE, Ames GM, Butterfield BJ, Cavender-Bares J, Firn J, Laughlin DC, Sutton-Grier AE, Williams L, Wright J (2017). Revisiting the Holy Grail: using plant functional traits to understand ecological processes. Biological Reviews, 92(2), 1156-1173. https://doi.org/10.1111/brv.12275.
15. Fan BL, Westerband AC, Wright IJ, Gao PF, Ding NN, Ai DX, Tian TT, Zhao X, Sun K (2023) Shifts in plant resource use strategies across climate and soil gradients in dryland steppe communities. Plant and Soil. https://doi.org /10.1007/s11104-023-06401-z.
16. He JL, Li XG (2016) *Potentilla fruticosa* has a greater capacity to translocate phosphorus from the lower to upper soils than herbaceous grasses in an alpine meadow. Agriculture, Ecosystems &

Environment, 228, 19-29. https://doi.org /10.1016/j.agee.2016.04.021.

17. Hacke UG, Sperry JS, Pittermann J (2000) Drought experience and cavitation resistance in six shrubs from the Great Basin, Utah. Basic & Applied Ecology, 1(1), 31-41. https://doi.org/10.1078/1439-1791-00006.
18. Hao GY, Sack L, Wang AY, Cao KF, Goldstein G (2010) Differentiation of leaf water flux and drought tolerance traits in hemiepiphytic and non-hemiepiphytic *Ficus* tree species. Functional Ecology, 24(4): 731-740. https://doi.org/10.111 1/j.13 65-2435.2010. 01724.x.
19. Han H, Xi BY, Wang Y, Feng JC, Li XM, David TT (2022) Lack of phenotypic plasticity in leaf hydraulics for 10 woody species common to urban forests of North China. Tree Physiology, 42(6), 1203-1215. https://doi.org/10.1093/tree phys/tpac003.
20. Jin Y, Wang CK, Zhou ZH, Li ZM (2016) Co-ordinated performance of leaf hydraulic and economics in 10 Chinese temperate tree species. Functional Plant Biology, 42, 1082–1090. http://doi.org/10.1071/FP16097.
21. Joshi J, Stocker BD, Hofhansl F, Zhou SX, Dieckmann U, Prentice IC (2022) Towards a unified theory of plant photosynthesis and hydraulics. Nature Plants, 8, 1304–1316. https://doi.org/10.1038/s41477-022-01244-5.
22. Kong DL, Wang JJ, Wu HF, Valverde-Barrantes OJ, Wang RL, Zeng H, Kardol P, Zhang HY, Feng YL (2019) Nonlinearity of root trait relationships and the root economics spectrum. Nature Communications, 10(1), 2203. https://doi.org /10.1038/s41467-019-10245-6.
23. Liu J, Gou XH, Liu JG, Yin DC, Zhang DY (2023) Comparative Analysis of the Drivers of Soil Organic Carbon, Total Nitrogen, and Phosphorus Stocks in Different Coniferous Plantations on the Eastern Tibetan Plateau. Journal of Soil Science and Plant Nutrition, 1-12. https://doi.org/10.1007/s42729-023-01540-9.
24. Liu H, Zhang Y, Xu X, Li SS, Wu JH, Li B, Nie M (2023) Root plasticity benefits a global invasive species in eutrophic coastal wetlands. Functional Ecology. https://doi.org/10.1111/1365-2435.14452.
25. Liao C, Clark PE, DeGloria SD (2018) Bush encroachment dynamics and rangeland management implications in southern Ethiopia. Ecology and Evolution, 8(23): 11694-11703. https://doi.org/10.1002/ece3.4621.
26. Li JL, Chen XP, Wu PP, Niklas KJ, Lu YM, Zhong QL, Hu DD, Cheng L, Cheng DL (2022) The fern economics spectrum is unaffected by the environment. Plant, Cell & Environment, 45(11): 3205-3218. https://doi.org/10. 1111/pce.144 28.
27. Li MY, Leng QN, Hao GY (2021) Contrasting patterns of radial growth rate between *Larix principis-rupprechtii* and *Pinus sylvestris var. mongolica* along an elevational gradient are mediated by differences in xylem hydraulics. Forest Ecology and Management, 497. https://doi.org/10.1016/j.foreco.2021.119524.
28. Liu H, Gleason SM, Hao G, He PC, Goldstein G, Ye Q (2019) Hydraulic traits are coordinated with maximum plant height at the global scale. Science Advances, 5(2).

http://doi.org/10.1126/sciadv.aav1332.

29. Liu R, Yang XJ, Gao RR, Huang ZY, Cornelissen JHC (2023) Coordination of economics spectra in leaf, stem and root within the genus Artemisia along a large environmental gradient in China. Global Ecology and Biogeography, 32(2), 324-338. https://doi.org/ 10.1111/geb.13624.
30. Liang XY, He PC, Liu H, Zhu SD, Uyehara IK, Hou H, Wu GL, Zhang H, You ZT, Xiao YY, Ye Q (2019) Precipitation has dominant influences on the variation of plant hydraulics of the native *Castanopsis fargesii* (Fagaceae) in subtropical China. Agricultural and Forest Meteorology, 271, 83-91. https://doi.org/10.1016/j.agr formet. 2019.02.043.
31. Li XY, Zhang SY, Peng HY, Hu X, Ma YJ (2013) Soil water and temperature dynamics in shrub-encroached grasslands and climatic implications: results from Inner Mongolia steppe ecosystem of north China. Agricultural and forest meteorology. 171, 20-30. https://doi.org/10.1016/j.agrformet.2012.11.001.
32. Li FL, Hu H, McCormlack ML, Feng FD, Liu X, Bao WK (2019) Community-level economics spectrum of fine-roots driven by nutrient limitations in subalpine forests. Journal of Ecology. 107(3), 1238-1249. https://doi.org/10.1111/1365-2745.13125.
33. Ma ZQ, Guo DL, Xu XL, Lu MZ, Bardgett RD, Eissenstat DM, McCormack ML, Hedin LO (2018) Evolutionary history resolves global organization of root functional traits. Nature,555(7694), 94-97. https://doi.org /10.1038/nature2578 3.
34. Medeiros JS, Burns JH, Nicholson J, et al. (2017) Decoupled leaf and root carbon economics is a key component in the ecological diversity and evolutionary divergence of deciduous and evergreen lineages of genus Rhododendron. American Journal of Botany, 104(6): 803-816. https://doi.org/10.3732/ajb.17 00051.
35. Maréchaux I, Bartlett MK, Sack L, Baraloto C, Engel J, Joetzjer E, Chave J (2015) Drought tolerance as predicted by leaf water potential at turgor loss point varies strongly across species within an Amazonian forest. Functional Ecology, 29, 1268-1277. https://doi.org/10.1111/1365-2435.12452.
36. Mediavilla S, Martín I, Escudero A (2020) Vein and stomatal traits in leaves of three co-occurring Quercus species differing in leaf life span. European Journal of Forest Research, 139, 829-840. https://doi.org/10.1007/s10342-020-01290-8.
37. Pritzkow C, Williamson V, Szota C, Trouvé R, Arndt SK (2020) Phenotypic plasticity and genetic adaptation of functional traits influences intra-specific variation in hydraulic efficiency and safety. Tree Physiology, 40(2), 215-229. https://doi. org/10.1093/treephys/tpz121.
38. Rosas T, Mencuccini M, Batlles C, Regalado I, Saura-Mas S, Sterck F, Martínez-Vilalta J (2021) Are leaf, stem and hydraulic traits good predictors of individual tree growth? Functional Ecology, 35(11), 2435-2447. https://doi. org/ 10.1111/1365-2435.13906.
39. Reich PB (2014) The world-wide 'fast–slow' plant economics spectrum: a traits manifesto. Journal of Ecology, 102(2), 275-301. https://doi.org/10.1111/136527 45.12211.
40. Santiago LS, De Guzman ME, Baraloto C, Vogenberg JE, Brodie M, Hérault B, Fortunel C, Bonal D (2018) Coordination and trade-offs among hydraulic safety, efficiency and drought avoidance traits

in Amazonian rainforest canopy tree species. New Phytologist, 218(3),1015-1024. https://doi.org/10.1111/nph.15 058.

41. Sperry JS, Donnelly JR, Tyree MT (1988) A method for measuring hydraulic conductivity and embolism in xylem. Plant, Cell & Environment, 11(1), 35-40. https://doi.org/10.11 11/j.1365-3040.1988.tb01774.x.
42. Silva JLA, Souza AF, Caliman A, Voigt EL, Lichston JE (2018) Weak whole-plant trait coordination in a seasonally dry South American stressful environment. Ecology and Evolution, 8(1), 4-12. https://doi.org/10.1002/ece3. 3547.
43. Wright IJ, Reich PB, Cornelissen JHC, Falster DS, Garnier E, Hikosaka K, Lamont BB, Lee W, Oleksyn J, Osada N, Poorter H, Villar R, Warton DI, Westoby M (2005) Assessing the generality of global leaf trait relationships. New phytologist, 166(2), 485-496. https://doi.org/10.1111/j.14698137.2005.01349.x.
44. Wright IJ, Reich PB, Westoby M, Ackerly DD, Baruch Z, Bongers F, Cavender-Bares J, Chapin T, Cornelissen JHC, Diemer M, Flexas J, Garnier E, Groom PK, Gulias J, Hikosaka K, Lamont BB et al (2004) The worldwide leaf economics spectrum. Nature, 428(6985), 821-827. https://doi.org/10.1038/natu re02403.
45. Wang XT, Nielsen UN, Yang XL, Zhang LM, Zhou XH, Du GZ, Li GX, Chen SY, Xiao S (2018). Grazing induces direct and indirect shrub effects on soil nematode communities. Soil Biology and Biochemistry, 121, 193-201. https://doi.org/ 10.1016/j.soilbio.2018.03.007.
46. Xu HY, Han WH, Prentice IC, Harrison SP, Wright IJ (2021) Coordination of plant hydraulic and photosynthetic traits: confronting optimality theory with field measurements. New Phytologist, 232(3), 1286-1296. https://doi.org/10.1111/ nph.17656.
47. Zhou Y, Ma HB, Lu Q, et al. (2024) Different responses of leaf and root economics spectrum to grazing time at the community level in desert steppe, China. Science of The Total Environment, 2024, 909: 168547. https://doi.org/10.1016/j.scito tenv.2023.168547.
48. Zhang A, Chen SY, Chen JW, Cui HW, Jiang XX, Xiao S, Wang JJ, Gao HN, An LZ, Cardoso P (2023) Shrub and precipitation interactions shape functional diversity of nematode communities on the Qinghai-Tibet Plateau. Global Change Biology. 29(10), 2746-2758. https://doi.org/10.1111/gcb.16638.
49. Zhu SD, Chen YJ, Ye Q, He PC, Liu H, Li RH, Fu PL, Jiang GF, Cao KF (2018) Leaf turgor loss point is correlated with drought tolerance and leaf carbon economics traits. Tree Physiology, 38(5), 658-663. https://doi.org/10.1093/tr eephys/tpy01 3.
50. Zhou T, Zhang W (2021) Anthropogenic warming of Tibetan Plateau and constrained future projection. Environmental Research Letters, 16(4):044039. http://doi.or g/10.1088 /1748-9326/abede8.

Figures

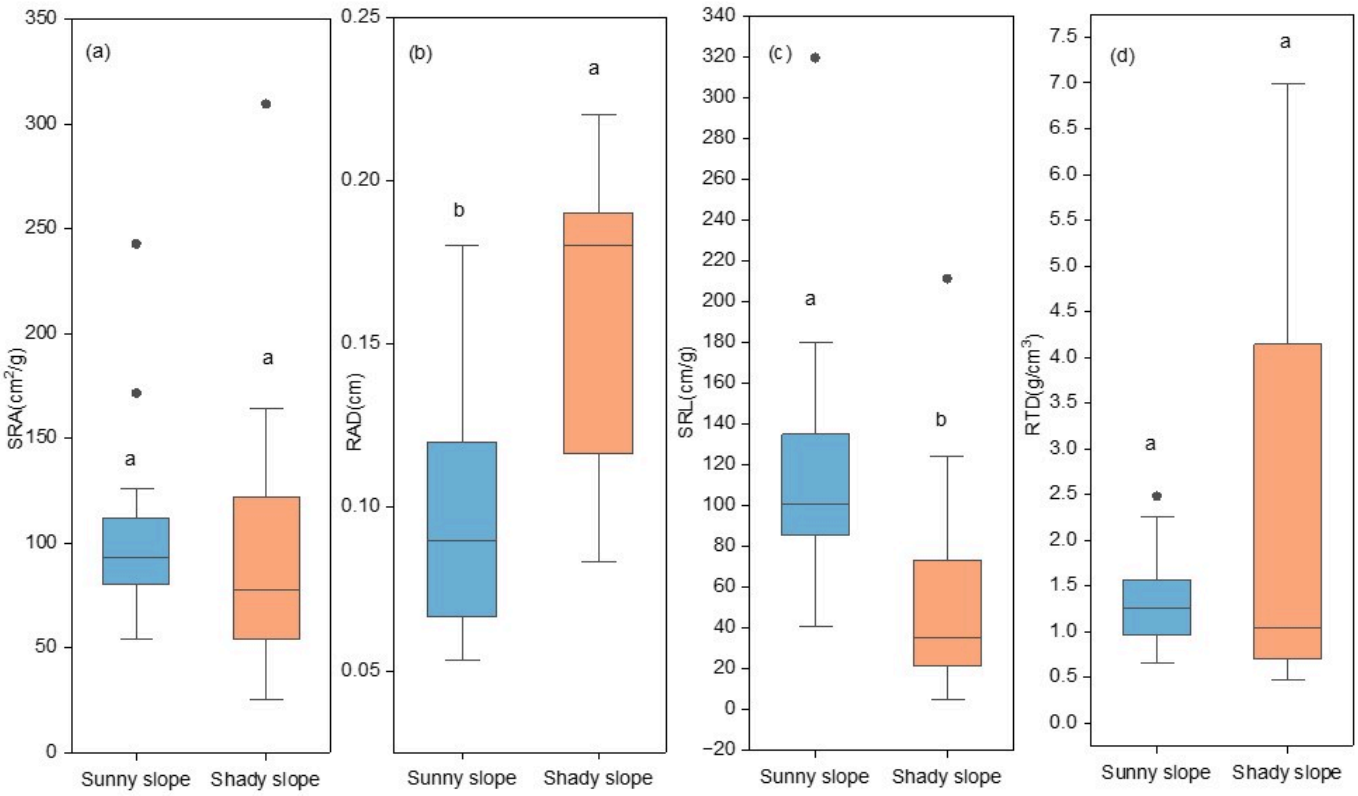

Figure 1

Comparisons of root functional traits of *D. fruticosa* between sunny and shady slopes (a) specific root area (SRA), (b) Root average diameter (RAD), (c) specific root length (SRL), (d) root tissue density (RTD)

Note: The top and bottom lines of the boxes represent the 25th and 75th percentiles, respectively, and the horizontal line in each box represents the median. The horizontal lines extending from the box represent the lowest and highest values within a range of 1.5× interquartile and the vertical line represents the 1.5×interquartile. The dots represent outliers. Date are from 4-5 replicates. Different lowercase letters indicate significant difference (p<0.05) or very significant difference (p<0.001)

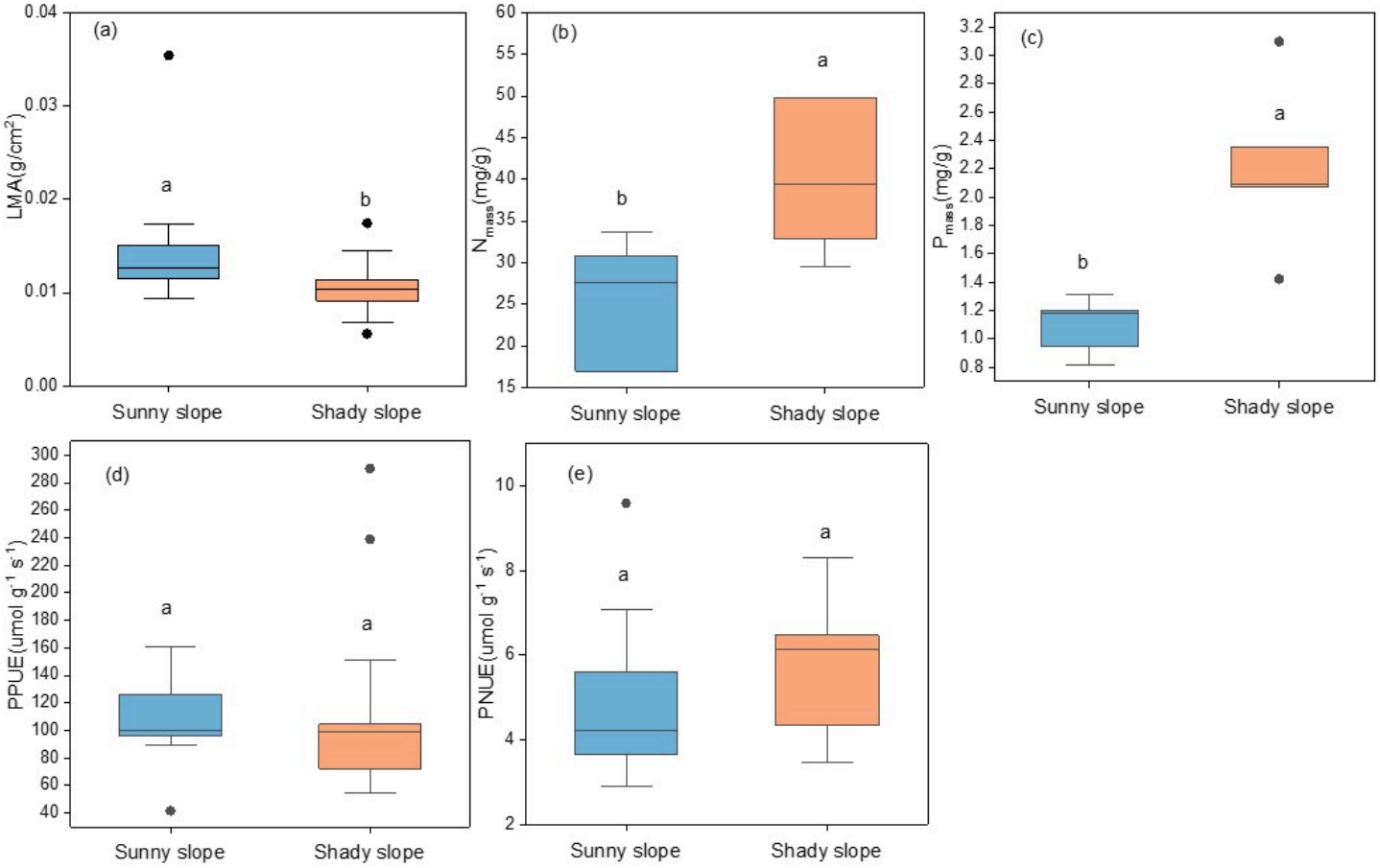

Figure 2

Comparisons of leaf functional traits of *D. fruticosa* between sunny and shady slopes. (a) leaf mass area (LMA), (b) Leaf nitrogen content (N_{mass}), (c) Leaf phosphorus content (P_{mass}), (d) Photosynthetic phosphorus use efficiency (PPUE), (e) Photosynthetic nitrogen use efficiency (PNUE)

Note: The top and bottom lines of the boxes represent the 25th and 75th percentiles, respectively, and the horizontal line in each box represents the median. The horizontal lines extending from the box represent the lowest and highest values within a range of 1.5× interquartile and the vertical line represents the 1.5×interquartile. The dots represent outliers. Date are from 4-5 replicates. Different lowercase letters indicate significant difference (p<0.05) or very significant difference (p<0.001).

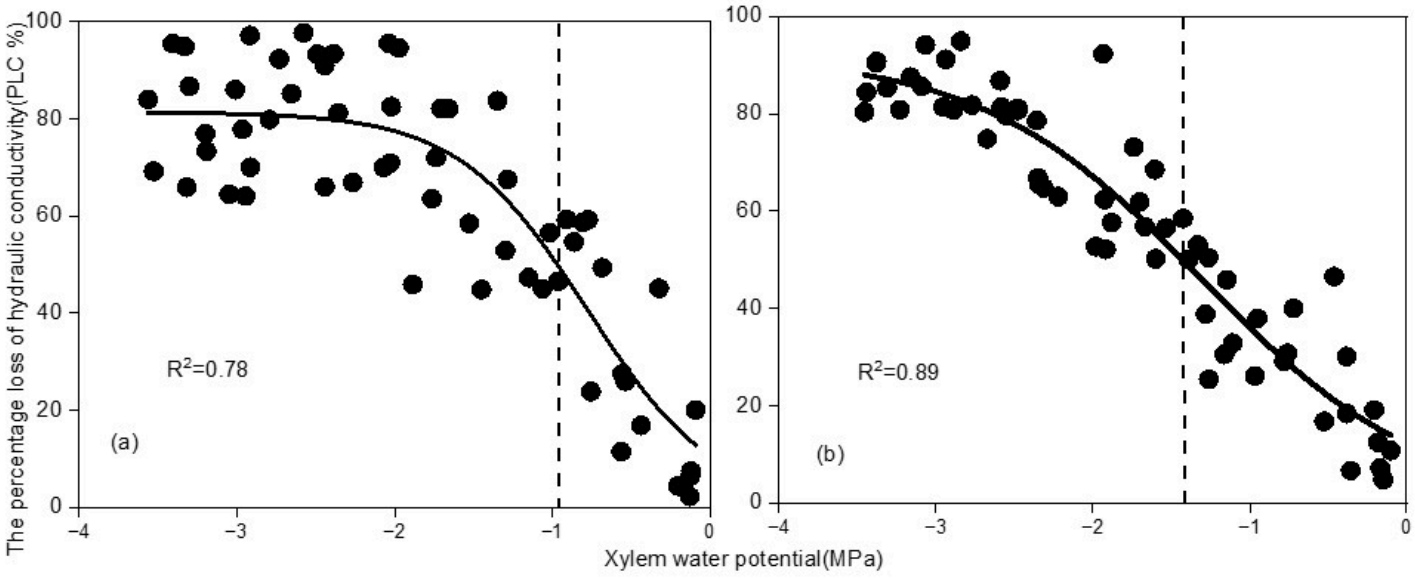

Figure 3

Stem vulnerability curves (VCs) for the shady (a) and sunny slopes (b). Vertical dashed lines show xylem water potential (Ψ_{leaf}) at 50 % loss of hydraulic conductivity

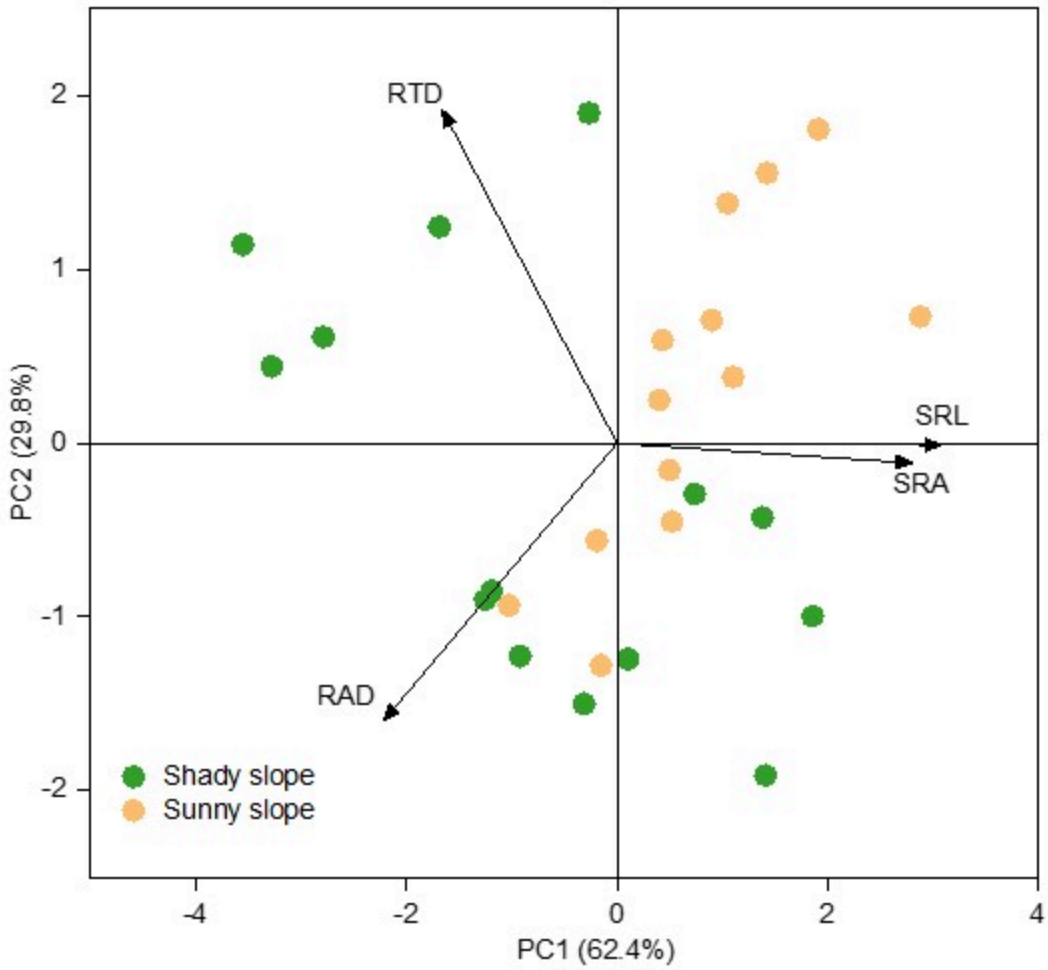

Figure 4

Principal components analysis (PCA) among fine-root functional traits.

See Abbreviations for fine-root functional traits.

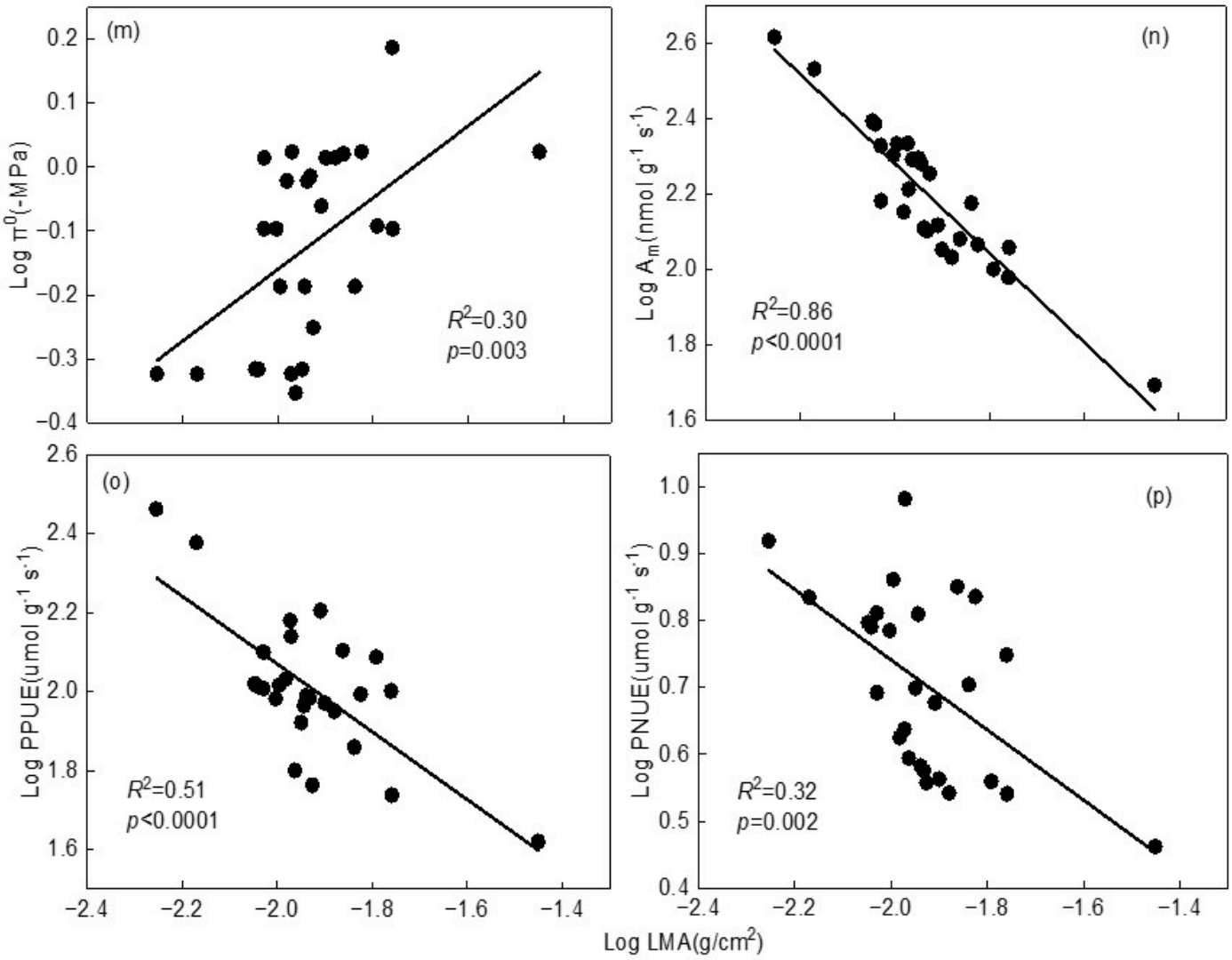

Figure 5

Linear regression relationship between root traits and stem and leaf hydraulic traits. (a-d) Correlations between SRL and SRA, RAD, RTD, P_{mass}; (e-h) Correlations between K_L and N_{mass}, P_{mass}, A_a, g_s; (i-l) Correlations between K_s and N_{mass}, P_{mass}, A_a, g_s; (m-p) Correlations between LMA and π^0, A_m, PPUE, PNUE. Line indicates best fit and R-values indicate correlation coefficients

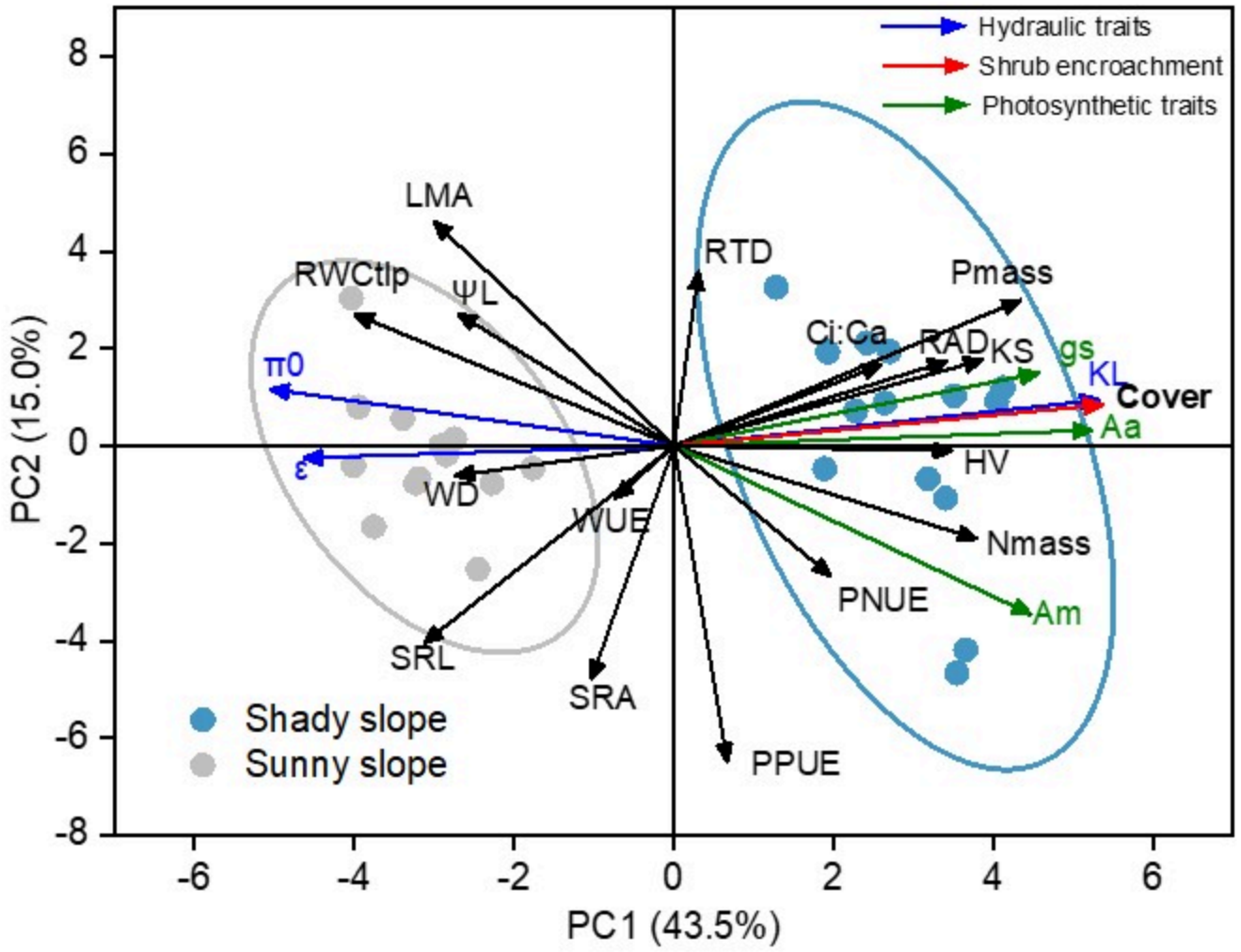

Figure 6

PCA ordination of shady slope and sunny slope on vegetation cover and all functional properties. The arrows show factor loadings of each variable on each axis, the dots denote the scores of PC1 (x axis) and PC2 (y axis), and the percentages of variance explained by the first two PCs are shown in the axis labels. Circles show the different habitats

Supplementary Files

This is a list of supplementary files associated with this preprint. Click to download.

- SupplementaryInformation.docx